Materials Today Bio 16 (2022) 100438

Contents lists available at ScienceDirect

Materials Today Bio

journal homepage: www.journals.elsevier.com/materials-today-bio

Coaxial TP/APR electrospun nanofibers for programmed controlling inflammation and promoting bone regeneration in periodontitis-related alveolar bone defect models

Ze He [a], Shibo Liu [a], Zhongming Li [b], Jiazhuang Xu [b], Yao Liu [a,**], En Luo [a,*]

[a] State Key Laboratory of Oral Diseases & National Clinical Research Center for Oral Diseases & Dept. of Oral and Maxillofacial Surgery, West China Hospital of Stomatology, Sichuan University, Chengdu, 610041, PR China
[b] College of Polymer Science and Engineering, State Key Laboratory of Polymer Materials Engineering, Sichuan University, Chengdu, 610065, PR China

ARTICLE INFO

Keywords:
Tissue engineering
Nanofibers
Bone regeneration
Inflammation
Periodontitis

ABSTRACT

Periodontitis is a pathological dental condition that damages the periodontal tissue and leads to tooth loss. Bone regeneration in periodontitis-related alveolar bone defects remains a challenge for periodontists and tissue engineers because of the complex periodontal microenvironment. The inflammatory microenvironment is associated with poor osteogenesis; therefore, the reduction of inflammation is essential for bone regeneration in periodontitis-related alveolar bone defects. Here, we developed a programmed core-shell nanofibers that allows the sequential and controlled release of tea polyphenols (TP) and AdipoRon (APR) to control inflammation and promote bone regeneration to repair periodontitis-related alveolar bone defects. Core-shell nanofibers with a sequentially controlled release function were synthesized using electrospinning. We investigated the therapeutic effects of the nanofibers *in vitro* and in a mouse periodontitis model. The results of the release profiles demonstrated that TP was released rapidly in the early stages and APR was continuously released thereafter. *In vitro* experiments showed that the programmed core-shell nanofibers reduced the levels of proinflammatory cytokines and increased osteogenic differentiation in an inflammatory microenvironment. In *vivo* experiments, the programmed core-shell nanofibers ameliorated periodontal tissue inflammation and improved alveolar bone regeneration. Our results indicated that the programmed core-shell nanofibers with a sequential-release function provides an ideal strategy for repairing periodontitis-related alveolar bone defects, and its application in the treatment of diseases with spatiotemporal specificity is promising.

1. Introduction

Periodontal disease is the most common oral disease, affecting up to 90% of the global population [1,2]. Progression to periodontitis results in the destruction of the alveolar bone clinically manifested as tooth loosening or pathological tooth loss [3]. Moreover, severe periodontitis can increase the risk of many chronic inflammatory systemic diseases, such as preterm birth and diabetes [4,5]. Treatment for periodontitis generally includes tooth scaling, root planning, and guided tissue regeneration [6]. However, current treatment methods are unsatisfactory for alveolar bone defects caused by periodontitis, and combined treatments are required [7,8]. Additionally, the inflammatory environment associated with periodontitis impairs the ability of cells to repair periodontal tissue, especially bone tissue [9,10]. Therefore, controlling inflammation and promoting bone regeneration are vital factors in the treatment of periodontitis-related alveolar bone defects [11]. Inhibition of the inflammatory process in the early stage plays an important role in maintaining a good microenvironment for alveolar bone regeneration. Therefore, the use of novel nanomaterials to sequentially control inflammation and promote tissue regeneration in periodontitis is worth investigating.

Electrospinning is an efficient technique for constructing polymeric nanofibers with superior physicochemical properties [12]. It is used to produce fibrous structures similar to the native extracellular matrix, which can be functionalized to carry inorganic substances, bioactive factors, or chemical drugs [13]. Electrospinning can be used in many biomedical fields, including sustained drug release and tissue engineering [14,15]. Owing to their outstanding biocompatibility and

* Corresponding author.
** Corresponding author.
E-mail addresses: letitialy@sina.com (Y. Liu), luoen521125@sina.com (E. Luo).

https://doi.org/10.1016/j.mtbio.2022.100438
Received 17 August 2022; Received in revised form 21 September 2022; Accepted 22 September 2022
Available online 22 September 2022

biodegradability, Poly lactic-*co*-glycolic acid (PLGA) and gelatin (GEL) are ideal materials for electrospinning [16,17]. GEL, a natural biological macromolecule, exhibits excellent hydrophilicity and is important for active cell-biomaterial interactions [18,19]. PLGA is a degradable functional polymer organic compound, and its degradation rate is lower than that of GEL [20].

At present, antibiotics such as minocycline and metronidazole are often used to control the inflammatory conditions of periodontitis [21,22]. However, antibiotics can induce drug resistance and are unsuitable for long-term use [23]. Tea polyphenols (TP) are active compounds present in tea and are mainly composed of catechins and their derivatives, which have a positive effect on periodontitis treatment [24,25]. Many studies have explored the therapeutic effect of TP on periodontitis, and the main therapeutic effect was found to be reflected by the inhibition of periodontal inflammation [26,27]. TP were also reported to prevent periodontal inflammation by decreasing the levels of interleukin-1(IL-1β) and tumor necrosis factor (TNF)-α, which are the major proinflammatory cytokines relevant to periodontal destruction [28,29]. AdipoRon (APR), an adiponectin mimetic, specifically binds to the adiponectin receptor and promotes alveolar bone regeneration by enhancing osteogenic differentiation [30]. We have previously demonstrated that APR inhibits bone resorption by suppressing osteoclast differentiation and function [31].

In this study, coaxial electrospinning was used to prepare electrospun nanofibers with APR in the core layer and TP in the shell layer. This study aimed to construct a sequential and controlled drug release system to coordinate the spatiotemporal specificity of the periodontitis bone remodeling process to effectively control inflammation and facilitate bone regeneration.

2. Materials and methods

2.1. Materials

GEL, hexafluoroisopropanol, dimethylformamide and dichloromethane were obtained from Sigma-Aldrich (St. Louis, MO, USA). PLGA (MW = 4 kDa, PLLA/PGA = 75:25) was obtained from Daigang Biomaterial Co., Ltd (Jinan, China). TP was obtained from Solarbio (Beijing, China). APR was purchased from Target Mol (Boston, USA). The TP detection kit was purchased from Leagene (Beijing, China). Lipopolysaccharide (LPS) was purchased from Sigma-Aldrich (St. Louis, MO, USA). Polystyrene tissue culture plates and Transwell systems were purchased from Corning (NY, USA).

2.2. Production of nanofibers

A 7.5% (w/v) GEL solution was obtained by dissolving GEL in hexafluoroisopropanol and stirring for 6 h. And a 20% (w/v) PLGA solution was obtained by dissolving PLGA in dichloromethane/dimethylformamide (v/v = 2.5:1) and stirring 6 h. To incorporate TP and APR into the nanofibers, 50 mg of TP was dissolved in 10 mL of GEL solution, and 10 mg of APR was dissolved in 5 mL of PLGA solution and sonicated for 1 h at 0 °C. The fluid flow rates of the outer and inner solutions were 0.5 and 0.25 mL/h, respectively. Electrospinning was performed at a voltage of 22 kV, and a 15 cm was set as the electrode distance. All processes for coaxial electrospinning were performed at 25 °C with 50 ± 5% humidity. The collected nanofibers were dried for 48 h in a vacuum oven to evaporate the residual organic solvent.

Four kinds of nanofibers were produced using coaxial electrospinning: PLGA/GEL, PLGA/GEL-TP, PLGA-APR/GEL, and PLGA-APR/GEL-TP. In the following experiment, PLGA/GEL, PLGA/GEL-TP, PLGA-APR/GEL, and PLGA-APR/GEL-TP were defined as control, TP, APR, TP/APR group, respectively. And group without nanofibers was defined as blank group.

2.3. Characterization of the nanofibers

The surface morphology of four kinds nanofibers were observed by scanning electron microscopy (SEM, FEI Hillsboro, USA). The core-shell structures of the four kinds nanofibers were verified by transmission electron microscopy (TEM, Hitachi H-600, Japan) and laser scanning confocal microscope (Olympus FV3000, Japan). A contact angle analyzer (DSA 100 Mk 2, Krciss GmbH, Germany) was used to characterized the water contact angle. The porosity of nanofibrous scaffolds was detected by Specific Surface and Aperture Analyzer (TriStarII3020 M, Micromertics, USA).

To detect the drug release of PLGA-APR/GEL-TP, 100 mg nanofibrous scaffolds were added to 10 mL of phosphate buffered saline (PBS) in a 37 °C incubator. 1 mL of the supernatant was collected and replaced by equivalent fresh PBS at designated time periods. The amount of TP was measured by a TP detection kit, and APR was measured by high performance liquid chromatography (Target Core-C18, MS Technologies, USA).

$$\text{The cumulative release of TP} \Big/ \text{APR}\ (\%) = \frac{V1\text{Cn} + V2\sum C(n-1)}{w} X100$$

V1 represents the entire volume of PBS and *V2* represents the replaced volume each time. *Cn* represents TP/APR concentration in the supernatant. *W* represents the total weight of TP/APR in the sample.

2.4. In vitro experiments

2.4.1. Cell culture

Bone marrow stromal cells (BMSCs) were harvested from 2-week-old male C57BL/6 mice. Briefly, the femurs and tibias were obtained and the ends of the femora were cut. After precipitate the marrow by centrifuge, the marrow was resuspended by low-glucose α-MEM (containing 10% FBS, 50 U/mL penicillin and 50 μg/mL streptomycin). BMSCs at passage 2 were used in this experiment. The macrophage cell line RAW 264.7 was obtained from ATCC and cultured according their protocol. The RAW 264.7 cells was maintained in complete DMEM (containing 10% FBS, 50 U/mL penicillin and 50 μg/mL streptomycin).

2.4.2. Live-dead staining

To examine the cytocompatibility of the nanofibers, we plated the BMSCs on nanofibers to perform the live-dead staining (Sigma-Aldrich, USA) and BMSCs were added to plates as the blank group. After incubated with the staining solution for 20–30 min, the samples were observed by a laser scanning confocal microscope (Olympus, FV3000, Japan). The experiments were performed in triplicate, and three random fields were chosen from each specimen for cell counting. The number of live/dead cells were counted via image J software.

2.4.3. Anti-inflammation and promote osteogenesis experiments

The effects of nanofibers on inflammation and osteogenesis in an inflammatory microenvironment were investigated by utilizing a 6-well Transwell system (pore size: 0.4 μm). RAW 264.7 cells were added to the nanofibers in the upper chamber at a concentration of $4 \times 10^4/cm^2$, and BMSCs were added to the nanofibers in the lower chamber at a concentration of $2 \times 10^4/cm^2$. The dimensions of the nanofibers were the same as the dimensions of culture plates. For the blank group, cells were added to chambers without nanofibers. LPS (1 μg/mL) was added to both chambers. After 12 h, the medium in the upper chamber was replaced by complete DMEM and the medium in the lower chamber was replaced by osteogenic medium (osteogenic components: 50 μM ascorbic acid, 10 mM β-sodium glycerol-phosphate and 100 nM dexamethasone). After incubation, samples were collected to detect the levels of inflammation and osteogenesis.

2.4.4. Intracellular reactive oxygen species (ROS) detection

To detect the effect of nanofibers on scavenging intracellular ROS, DCFH-DA staining (Beyotime, China) was used. Briefly, after RAW 264.7 cells cocultured with LPS and nanofibers for 24 h, DCFH-DA was used to incubate the samples for 30 min, then the live RAW 264.7 cells were stained by using Hoechst 33342 solution (Beyotime, China). For the blank group, RAW 264.7 cells were added to the plates. The results were detected by laser scanning confocal microscope at 485 nm.

2.4.5. Osteoclastic differentiation experiments

RAW 264.7 cells were inoculated on nanofibers and cultured as we described before [32]. The samples were collected after 7 days and subjected to osteoclastic differentiation staining. Tartrate-resistant acid phosphatase (TRAP) staining (Sigma-Aldrich, USA) and F-actin immunofluorescence staining was applied following according to the manufacturer's protocol. Moreover, TRAP-positive cells with no fewer than three nuclei were regarded as osteoclasts.

2.4.6. Immunofluorescence staining

The samples were fixed with 4% paraformaldehyde, followed by incubation with 1% Triton X-100 and 3% BSA. Subsequently, the related primary antibody (Runx2, ab23981, Abcam, UK) were used to incubated with the samples overnight. After that, secondary antibody was utilizing to incubate the samples before staining with FITC-labeled phalloidin and DAPI. The samples were observed by laser scanning confocal microscope.

2.4.7. Alkaline phosphatase (ALP) staining

To explore the effect of PLGA-APR/GEL-TP on osteogenic differentiation under inflammatory environment, ALP staining was performed. Briefly, the samples were fixed with 4% paraformaldehyde, followed by incubation with ALP staining Kit (Beyotime, China). The quantitative analysis of ALP activity was also performed according to the protocol of the ALP assay kit (Beyotime, China). Briefly, after induction for 7 days, the samples were lysed in lysis buffer containing 0.1% Triton X-100 and the supernatant were collected after centrifugation. The absorbance (405 nm) was measured to determine the ALP concentration by a microplate reader. The ALP activity was calculated and defined as nmol/assay time/mg protein.

2.4.8. Quantitative real-time polymerase chain reaction (qRT-PCR) and western blotting

In order to assess the gene expression of inflammatory cytokines and osteogenic-related factors, qRT-PCR was applied as we described before [32]. The primers are listed in Table 1.

To explore the osteogenic differentiation of BMSCs under inflammatory conditions, the protein expression of Col I, Runx2, OCN and OPN was determined by western blot analysis as we previously described [32]. Anti-Col I (ab21286, Abcam, UK), anti-Runx2 (ab236639, Abcam, UK), anti-OPN (ab283656, Abcam, UK) and anti-OCN (ab93876, Abcam, UK) primary antibodies were used in this study.

2.5. In vivo experiments

2.5.1. Periodontitis model

The surgical procedures were reviewed and approved by the West China Hospital of Stomatology Ethics Committee (WCHSIRB-D-2020-129) and complied with the ARRIVE guidelines. Sixty 8-week-old male C57BL/6 mice were obtained from laboratory animal center (Sichuan university) and fasten 20–25 °C ambient temperature. The mice were free to access to food and water prior and after experiments. Animal welfare was ensured by weekly single-cage control provided by the university authorized veterinarians staff. Animals were randomly assigned to five groups (n = 12 per group), considering that each animal had bilateral sides. Silk ligature was used to induce periodontitis in mice. After anesthetization, a 6-0 silk suture was placed around the maxillary second molar and tied. After 2 weeks, the ligature was removed and the periodontal pocket was rinsed with saline to remove accumulated food debris; after that, nanofibers of the same size (2 mm in width, 2 mm in length) were placed in the periodontal pocket. For the blank group, no material was placed in the periodontitis socket. Mice were sacrificed under excessive anesthesia at 1, 2, and 4 weeks after surgery. Bone tissue near the maxillary second molar was harvested for western blotting to examine the osteogenesis activity. Maxillae were harvested for micro-computed tomography (micro-CT) scanning and histology staining for further analysis.

Table 1
Primers used for qRT-PCR.

Gene	Forward Primer	Reverse Primer
GADPH	AGGTCGGTGTGTGAACGGATTTG	TGTAGACCATGTAGTTGAGGTCA
IL-1β	TGGAGAGTGTGGATCCCAAG	GGTGCTGATGTACCAGTTGG
TNF-α	CTGAACTTCGGGGTGATCGG	GGCTTGTCACTCGAATTTTGAGA
ALP	CCAACTCTTTTGTGCCAGAGA	GGCTACATTGGTGTTGAGCTTTT
OPN	CAGGGAGGCAGTGACTCTTC	AGTGTGGAAAGTGTGGCGTT
Runx 2	TTCAACGATCTGAGATTTGTGGG	GGATGAGGAATGCGCCCTA

2.5.2. Micro-CT scanning

Micro-CT (μ-CT40, SCANCO, Switzerland) was used to scan the samples with 10 μm pixel size and 70 kV operating voltage. Three-dimensional reconstruction and data evaluation were performed using SCANCO Medical Evaluation software. The range of interest (ROI): the anterior boundary was the distal side of the first molar, the posterior boundary is the mesial side of the third molar, and the buccal and lingual boundaries was the inner sides of buccal and lingual bone cortex, respectively [33]. The cementoenamel junction of the second molar was defined as the upper boundary and the 60 slides from the upper boundary was defined as lower boundary, the crown and root of the tooth were excluded. The ratio of bone volume to tissue volume (BV/TV), trabecular thickness (Tb·Th) and trabecular separation (Tb.Sp) were quantitatively analyzed. The mesial, middle, and distal of the buccal and palatal sides of the maxillary second molar were selected, and the distance between the cementoenamel junction and alveolar bone crest was measured to evaluate the bone resorption.

2.5.3. Histology staining

The maxillae were used for histology staining as we previously described [32]. Hematoxylin and eosin (H&E) staining, Masson staining and Trap staining were performed. For the immunohistochemical staining of macrophages, the samples were incubated with anti-iNOS (ab115819, Abcam) primary antibodies overnight. Afterwards, the secondary antibody (CST, USA) was incubated. To quantify the positive cells, three separate areas near the periodontium of the second molar for each sample were randomly selected.

2.5.4. ELISA

An ELISA kit (Sigma-Aldrich, USA) was utilized to examine the concentrations of IL-1β and TNF-α in the serum, following the manufacturer's instructions. Briefly, the blood was collected from mice by excising the eyeballs. After the blood coagulated naturally for 10 min, it was centrifuged for 15 min (3000 rpm), and the supernatant was harvested for further testing.

2.6. Statistical analysis

Data are shown as the mean ± SD. Significant differences were evaluated by one-way analysis of variance (ANOVA) with Tukey's post-hoc test for multiple comparisons using SPSS software. Statistical significance was set as $P < 0.05$, and all experiments were performed at least three times.

3. Results

3.1. Characterization of the programmed delivery system and in vitro drug release

3.1.1. PLGA-APR/GEL-TP shows a typical coaxial form

At present study, TP/APR programmed delivery system has been successfully synthesized by coaxial electrospinning. SEM images showed the nanofibers were continuous and interconnected. In the four groups, the diameters of the nanofibers were almost comparable, with the most frequent diameters ranging from 200 nm to 400 nm (Fig. 1C). As shown in Fig. 1B, the images of TEM exhibited a typical core-shell structure in each group, indicating that embedding TP and APR did not affect the coaxial structure. The nanofibers were observed under laser scanning

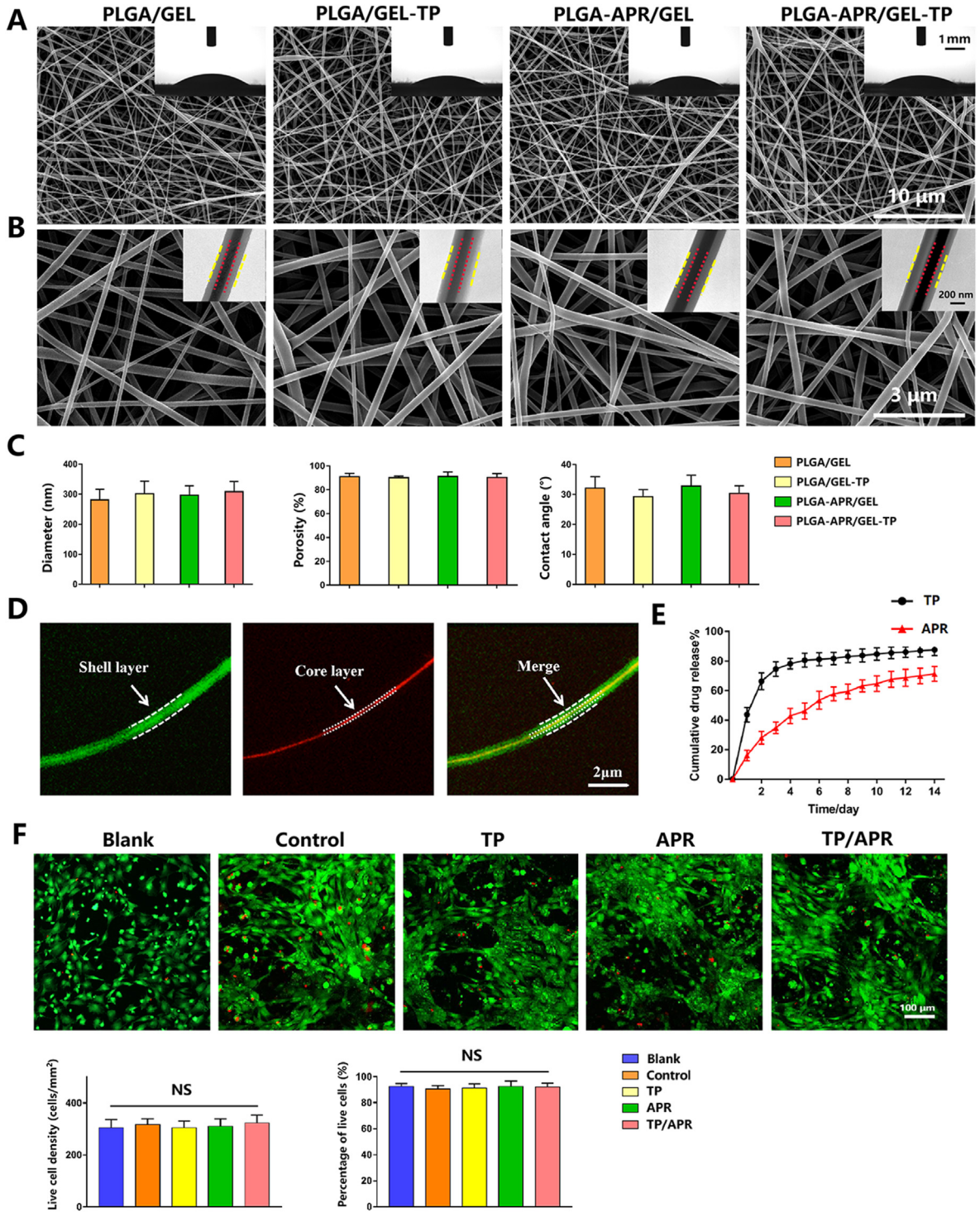

Fig. 1. Characterization of the nanofibers. (A) Scanning electron microscopy (SEM) images at 10000 × magnification; the inserts are water contact angle images. (B) SEM images at 40000 × magnification, the inserts are transmission electron microscopy images. (C) The histograms show the diameter, porosity, and contact angle of electrospun fibers. (D) Images of PLGA-rhodamine/GEL-calcein taken using a confocal microscope. (E) *In vitro* cumulative drug release profiles of PLGA-TP/GEL-APR nanofibers. (F) Fluorescence microscopy images of BMSCs cultured on nanofibers for 3 days *in vitro* and quantitative analysis (n = 3).

confocal microscope to verify that the substances carried by PLGA and GEL were distributed in the core and shell layers, respectively. The red dye (rhodamine) was gathered in the core, whereas the green dye (calcein) was distributed in the shell (Fig. 1D), demonstrated a good distribution of the two different substances. The contact angles of the nanofibers were relatively low and demonstrated a good hydrophilicity. The porosity of the nanofibers, which is an important parameter for biomaterials in nutrition transport, was relatively high (Fig. 1C).

3.1.2. PLGA-APR/GEL-TP exhibits a sequential and controlled release behavior

The cumulative release curves for TP and APR are shown in Fig. 1E. The PLGA-TP/GEL-APR exhibited a short burst release of TP in the early phase and a slow release over the following 14 days. The cumulative release rate of TP was 87.6 ± 3.1%, while that of APR was slow and stable, with a small burst release of 16.1 ± 2.9% on day 1 and a relatively sustained release in the following 14 days, reaching a cumulative release of 71.3 ± 4.1%. Hence, the release behavior of TP was faster than that of APR.

3.1.3. PLGA-APR/GEL-TP displays good cytocompatibility

Most BMSCs were alive and well spread, and little dead cells were detected (Fig. 1F). Quantitative analysis indicated that no statistical differences were observed in proliferation among the five groups on day 3. This result indicated that the programmed delivery system had outstanding cytocompatibility.

3.2. In vitro behavior of the programmed delivery system

As reported previously, the osteogenic capacity of BMSCs is highly damaged under inflammatory conditions [34,35]. Therefore, we designed a Transwell system to explore the effects of the programmed delivery system on the osteogenic differentiation of BMSCs in an inflammatory environment.

3.2.1. PLGA-APR/GEL-TP inhibits inflammation

TP/APR and TP group significantly decreased the inflammatory cytokines compared with the blank group (Fig. 2A). Inflammatory markers were also downregulated in APR group on day 4, which might be due to

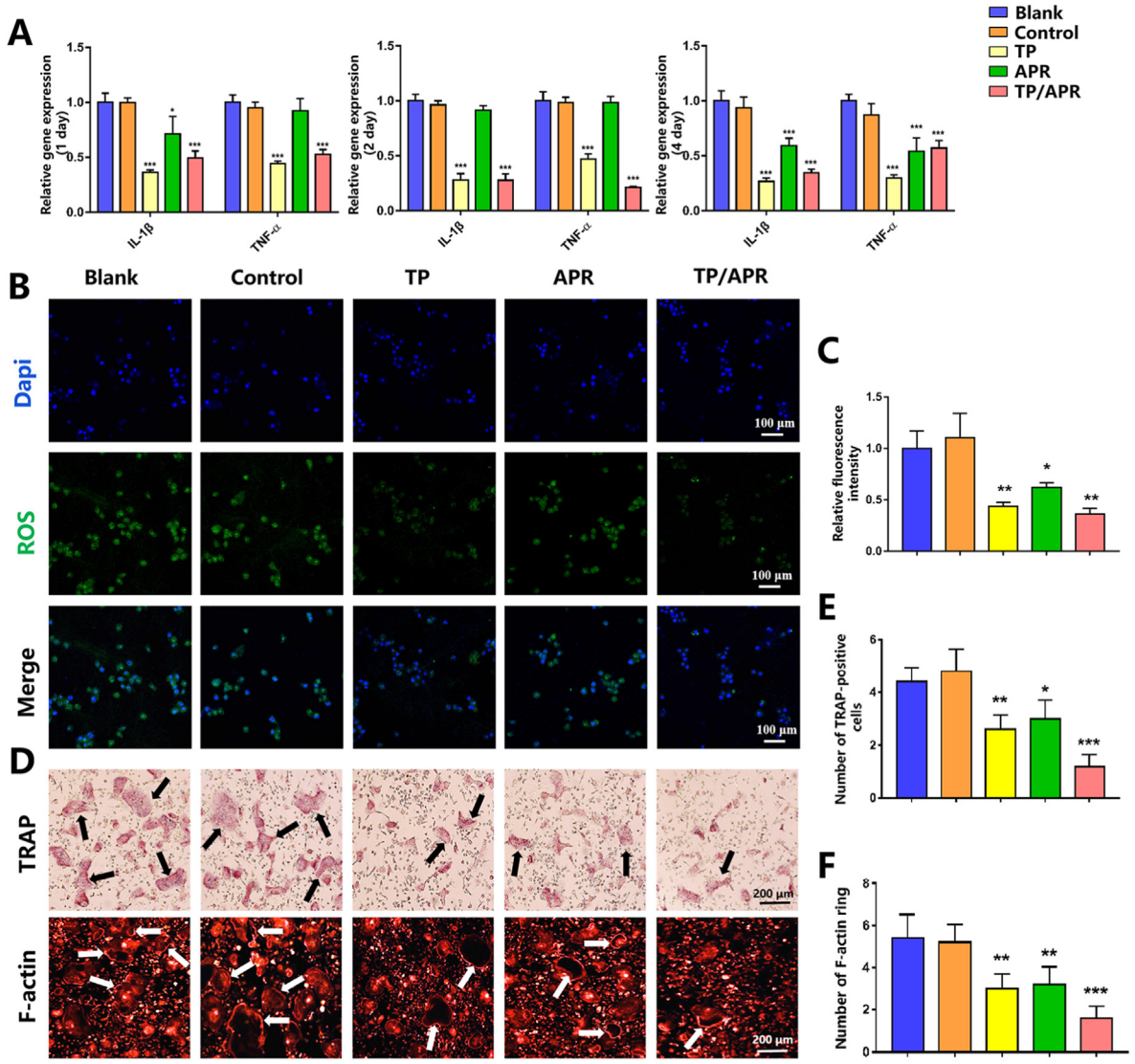

Fig. 2. The programmed delivery system inhibited inflammation and reduced osteoclastogenesis activity. (A) Inflammatory gene expression in RAW 264.7 cells was analyzed by qRT-PCR (n = 3). (B) Images of reactive oxygen species (ROS) levels detected by DCFH-DA staining (n = 3). (C) Relative fluorescence intensity of ROS (n = 3). (D) Representative images of TRAP and F-actin staining; the black arrows indicate the TRAP-positive osteoclasts and the white arrows show the F-actin rings (n = 3). (E) Quantitative analysis of TRAP-positive cells (n = 3). (F) Quantitative analysis of F-actin rings (n = 3). *$P < 0.05$, **$P < 0.01$ and ***$P < 0.001$, compared with the blank group.

the longer time required for APR release. Besides, the intracellular level of ROS was detected by DCFH-DA probe. As an important factor of aggravate inflammation, the overproduction of ROS can delay the periodontal tissue regeneration [36]. Therefore, reducing the ROS production in periodontal tissue might be considered essential to promote tissue regeneration. The results showed that RAW 264.7 cells cocultured with PLGA-APR/GEL-TP and PLGA/GEL-TP exhibited lower expression of ROS than others (Fig. 2B). These results demonstrated that outstanding anti-inflammation effects of nanofibers incorporated with TP.

3.2.2. PLGA-APR/GEL-TP decreases osteoclastogenesis activity

To further verify the programmed delivery system, we performed TRAP staining to investigate osteoclastogenesis in different groups. Compared to other groups, there were fewer TRAP-positive cells in the TP/APR group (Fig. 2D). Consistently, immunofluorescence staining results exhibited a significantly reduced number of F-actin rings in the TP/APR group. The results of the osteoclastogenic assay suggested that TP/APR inhibited osteoclast formation.

3.2.3. PLGA-APR/GEL-TP promotes osteogenic mineralization in an inflammatory environment

First, we examined the expression of typical osteogenic protein Runx2 of BMSCs. The results of immunofluorescence staining showed that BMSCs on PLGA-APR/GEL-TP showed most higher expression of osteogenic protein than others (Fig. 3A). Besides, higher ALP precipitation was detected in TP/APR group than in other groups (Fig. 3D). Quantitative results showed the same tendency, indicating that TP/APR group exhibited greater osteogenic differentiation. Consistent with these findings, qRT-PCR results (Fig. 3C) showed significantly higher osteogenic-related gene expression in the TP/APR group on days 4 and 7. Western blot results revealed the same trend, and higher levels of osteogenic proteins were observed in the TP/APR group (Fig. 3E).

Collectively, the results of *in vitro* experiments suggested that nanofibers incorporated with TP significantly prevent inflammation and that nanofibers incorporated with APR can improve the osteogenic activity of BMSCs when inflammatory cytokines are deceased.

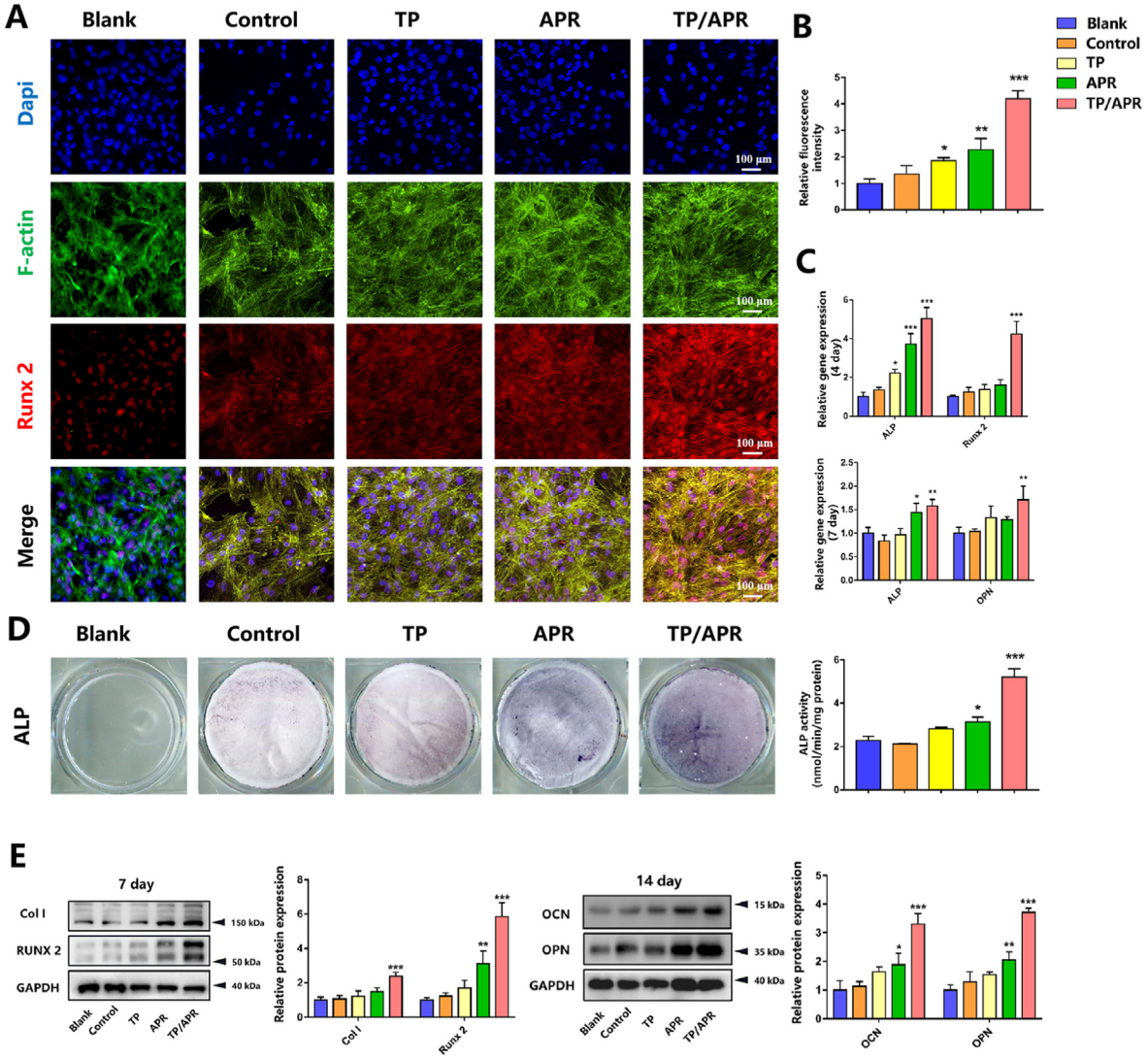

Fig. 3. The programmed delivery system promoted osteogenic mineralization in an inflammatory environment *in vitro*. (A) Images of immunofluorescence staining showing the expression of Runx2 of BMSCs (n = 3). (B) Corresponding quantitative results (n = 3). (C) Osteogenic gene expression in BMSCs, analyzed by qRT-PCR (n = 3). (D) Representative images and quantitative analysis of alkaline phosphatase staining (n = 3). (E) Western blot of Col I, Runx2, OCN, and OPN expression in BMSCs and statistical analysis (n = 3). *$P < 0.05$, **$P < 0.01$ and ***$P < 0.001$, compared with the blank group.

3.3. Programmed delivery system decreases inflammation and promotes bone regeneration in vivo

Based on the findings stated above, we hypothesized that the programmed delivery system could decrease inflammation and promote bone regeneration *in vivo*.

3.3.1. Micro-CT analysis

The bone parameters of periodontitis compared with those of normal periodontal bone in mice are shown in Fig. 4. Three-dimensional (3D) images revealed that the surface of the periodontal bone was uneven in the first week, particularly in the control and blank groups (Fig. 5A). The bone surface in the TP/APR group was flatter than that in the single drug-loaded groups. At 4 weeks, the smoothest surface and the highest alveolar ridge height were shown in the TP/APR group. Quantitative analysis confirmed that the TP/APR group had the highest BV/TV and Tb. N and lowest Tb.Sp among all groups, which were similar to the bone parameters of healthy periodontal bone tissue. The results of the quantitative analysis of alveolar bone resorption are shown in Fig. 5; the resorption height of alveolar bone in the TP/APR and TP groups was lower than that in other groups at week one. At 4 weeks, the TP/APR, APR, and TP groups exhibited better alveolar ridge height than that in other groups, and the TP/APR group showed the best alveolar ridge height. In the blank and control groups, resorption height worsened over time. Alveolar bone height was considerably recovered in the TP/APR group.

3.3.2. Histological evaluation

Histology staining was applied to further evaluate the alveolar bone regeneration. More bone tissue was observed in the TP/APR group, whereas there were extremely limited alveolar ridge in the control and blank groups (Fig. 6A). In the TP and APR groups, a moderate amount of alveolar ridges was observed, possibly due to the inhibition of bone resorption. Masson staining was used to detect the condition of the periodontal ligament near the second molar. The structure of the periodontal ligament degenerated into a sparse form in the blank group (Fig. 6B). However, the structure of the periodontal ligament was denser and contained more collagen fibers in the TP/APR group than in the control groups. TRAP staining showed that the level of osteoclast activity in the control and blank groups was higher, while the positive marks in the TP/APR group were the lowest. Additionally, fewer iNOS-positive macrophages were observed in the TP/APR group (Fig. 6C), indicating that the release of both TP and APR inhibited inflammation, particularly TP. No significant drug toxicity-related injury was found in animal organ samples (Fig. S2).

3.3.3. ELISA and WB evaluation

ELISA results of the serum confirmed the anti-inflammatory effects of TP/APR programmed delivery system (Fig. 6F). WB results of the alveolar bone demonstrated that TP/APR programmed delivery system promoted osteogenesis around the periodontium (Fig. 6G).

4. Discussion

Despite great progress in bone regeneration technology in recent years, periodontitis-related alveolar bone defects remain challenging due to the complexity of the periodontal microenvironment [37]. Uncontrolled inflammation is associated with poor osteogenesis; therefore, inhibition of inflammation to create a good environment for bone regeneration is important [3]. In this experiment, a programmed TP/APR sequential-release system using coaxial electrospinning was successfully synthesized.

Recently, electrospinning combined with different bioactive molecules for the locally controlled release of drugs has gained attention [38,39]. Wu et al. developed a scaffold loaded with BMP2 and dexamethasone to synergistically facilitate bone formation in a critically sized calvarial bone defect model [40]. Additionally, we have previously shown that nanofibers loaded with substance P and alendronate promote bone formation around dental implants [32]. While previous studies have mainly focused on osteogenesis, we speculated that utilizing the sequential and controlled release function of coaxial electrospun nanofibers fits the disease with spatiotemporal specificity. Therefore, inspired by the spatiotemporal specificity of periodontitis-related bone

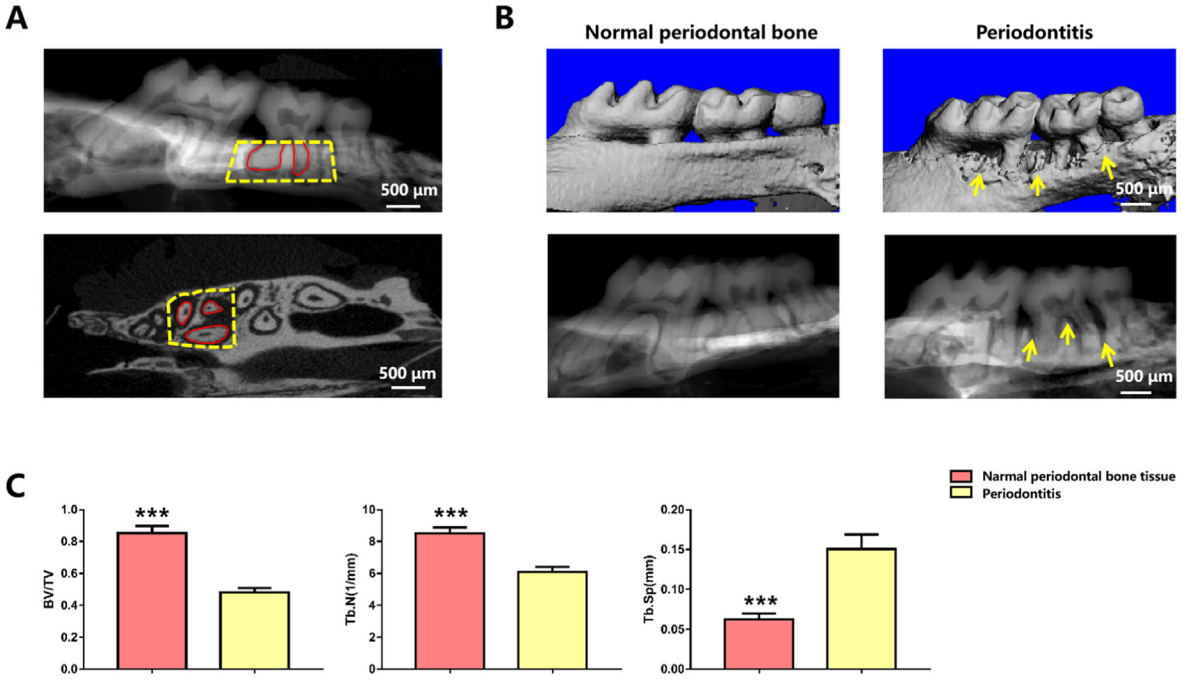

Fig. 4. Schematic illustration of ROI and the characteristics of alveolar bone in periodontitis. (A) Schematic illustration of ROI, the yellow dotted boxes show the ROI and the red line shows that the root of the tooth was excluded from the ROI. (B) Micro-CT images of the periodontal bone tissue after 2 weeks of suturing. (C) Comparison of bone parameters between periodontitis and normal periodontal bone tissue (n = 3). (***: $P < 0.001$). (For interpretation of the references to colour in this figure legend, the reader is referred to the Web version of this article.)

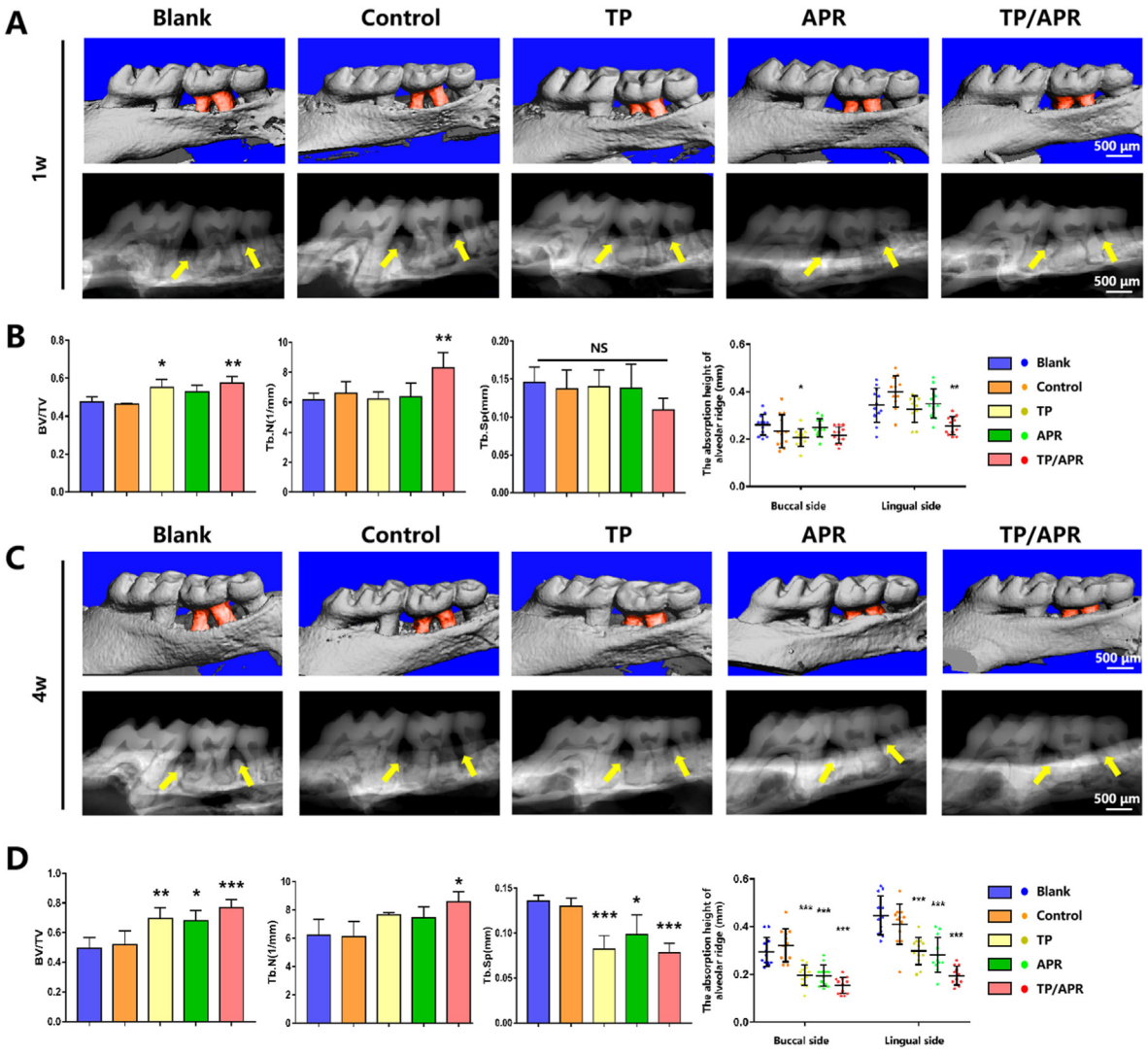

Fig. 5. The programmed delivery system significantly protected alveolar bone resorption and promoted bone regeneration *in vivo*. (A) Micro-CT images of periodontal bone tissue at 1 week. The red part displays the exposure of the tooth root, and the yellow arrows show the alveolar ridge. (B) Quantitative analysis of BV/TV, Tb·Th, and Tb.Sp, and quantitative analysis of absorption height of alveolar ridge at 1 week (n = 5). (C) Micro-CT images of periodontal bone tissue at 4 weeks. The red part shows the exposure of the tooth root, and the yellow arrows show the alveolar ridge. (D) Quantitative analysis of BV/TV, Tb·Th, and Tb.Sp, and quantitative analysis of absorption height of alveolar ridge at 4 weeks (n = 5). *P < 0.05, **P < 0.01 and ***P < 0.001, compared with the blank group. (For interpretation of the references to colour in this figure legend, the reader is referred to the Web version of this article.)

remodeling, we designed a sequential and controlled release system to inhibit inflammation and reduce bone resorption in the early stage and facilitate bone regeneration in the later stage.

In this study, nanofibers with core-shell structures were constructed, which formed the basis of the sequential-release system. PLGA and gelatin are ideal materials for electrospinning because of their good biocompatibility and biodegradability [41]. As a natural biological macromolecule, gelatin exhibits excellent hydrophilicity, and thus, it was selected as the shell layer to improve the hydrophobic property of the nanofibers [42]. PLGA is a degradable functional polymer organic compound, and its degradation rate is slower than that of gelatin, and thus, we chose it to form the core layer [43]. The contact angle test in this study showed that the nanofibers had good hydrophilicity, which is important for active cell-biomaterial interactions [44]. In the TP-APR sequential-release system, TP was released at a faster rate during the early stage and APR maintained a slow and stable release rate over the entire process. The release profile of PLGA-APR/gelatin-TP suggested that the different release rates of TP and APR mainly depend on the different degradation characteristics of gelatin and PLGA and the core-shell structure of the nanofibers. The sequential delivery of TP and APR could perfectly match the specificity of bone regeneration in periodontitis-related alveolar bone defects and might be an effective strategy to improve the treatment efficiency.

The inflammatory microenvironment impairs the osteogenic capacity of BMSCs; therefore, the inhibition or reduction of inflammation is essential for bone regeneration in periodontitis-related alveolar bone defects [9,45]. A previous study showed that TP effectively attenuates inflammation [46]. Consistently, our study showed that the initial burst release of TP has a strong inhibitory effect on inflammation and that the sustained release of APR also ameliorates the inflammatory conditions. Moreover, the combination of TP and APR inhibits osteoclast formation. The inhibition of inflammation and bone resorption creates a favorable environment for subsequent osteogenesis. In our previous study, APR was suggested to promote osteogenesis and enhance cell migration [31]. Furthermore, Wu et al. reported that APR could enhance osteogenic differentiation in a T2D-associated periodontitis model [30]. Thus, excellent osteogenic differentiation of BMSCs was observed under the influence of APR released in the later phase.

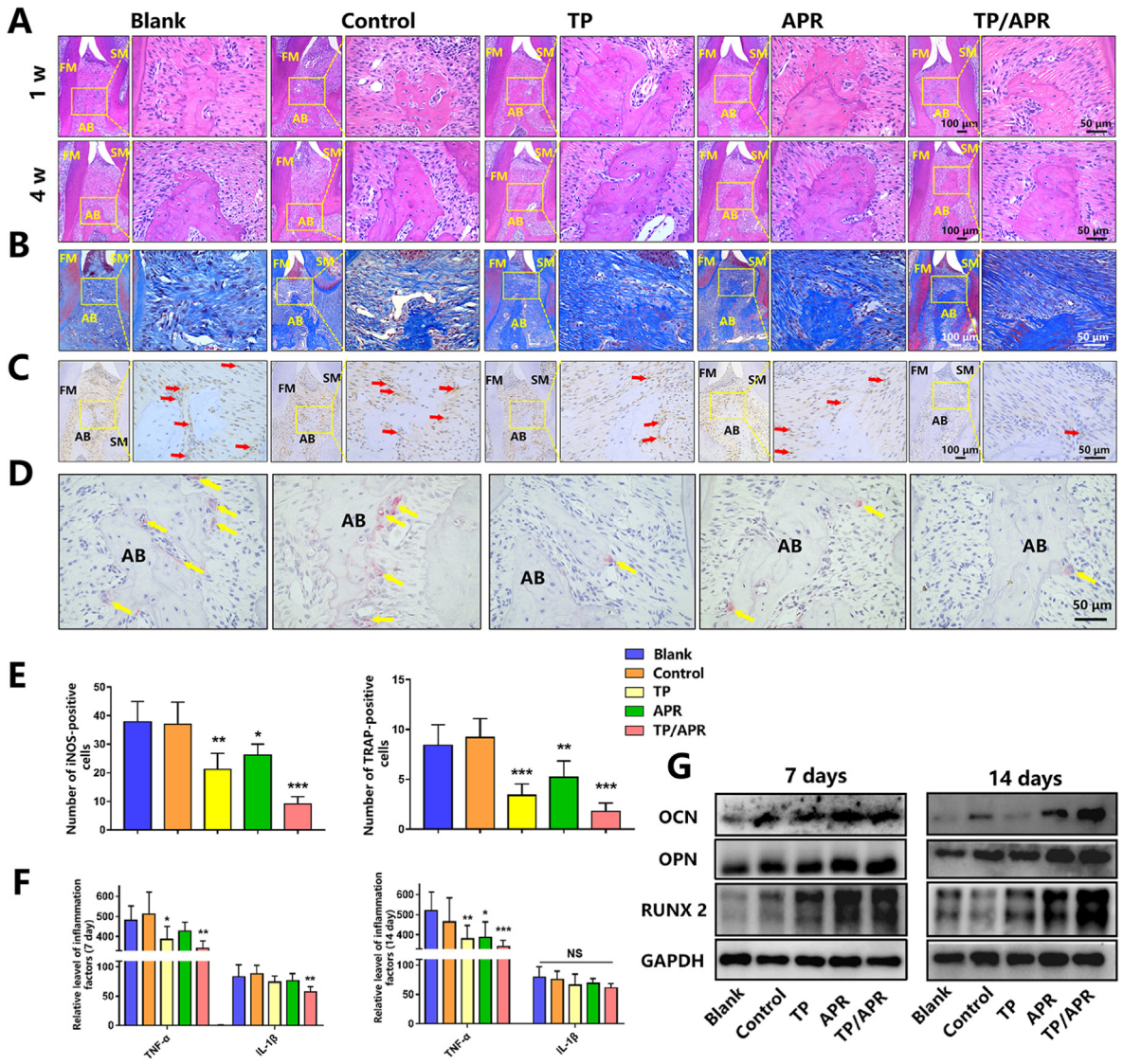

Fig. 6. The programmed delivery system obviously reduced the inflammation of periodontitis and enhanced bone regeneration *in vivo*. (A) Representative images of H&E staining at 1 and 4 weeks. (B) Representative images of Masson staining at 1 week. (C) Representative images of immunohistochemistry staining at 1 week; the red arrow indicates iNOS-positive cells. (D) Representative images of TRAP staining at 1 week; the yellow arrow indicates osteoclasts. (E) Quantitative analysis of iNOS-positive cells and TRAP-positive cells (n = 5). (F) The Relative levels of inflammatory cytokines in the serum at 1 and 2 weeks (n = 5). (G) Western blot of periodontal bone tissue near the second molar at 1 and 2 weeks. $^{*}P < 0.05$, $^{**}P < 0.01$ and $^{***}P < 0.001$, compared with the blank group; FM = first molar; SM = second molar; AB = alveolar bone. (For interpretation of the references to colour in this figure legend, the reader is referred to the Web version of this article.)

Periodontitis-related alveolar bone defect repairing is a complex and dynamic process, and multiple cells sense signals and play important roles in different periods [47]. In the early stage of the periodontitis, macrophages assemble and mediated the immune response [48]. Macrophages can be categorized into pro-inflammatory M1 and anti-inflammatory M2 types under different stimuli. M1-type macrophages highly express inflammatory cytokines, such as TNF-α and IL-1β, whereas M2-type macrophages participate in tissue repair and regeneration and express arginase-1 and IL-10 [49,50]. Under LPS stimulation conditions, macrophages become polarized to the M1-type and secrete inflammatory factors, which accelerates the progression of periodontitis [51]. Influenced by the inflammatory cytokines secreted by macrophages, the migration and osteogenic activity of BMSCs are inhibited [52]. Therefore, it is necessary to restore osteoimmune homeostasis at the initial stage of inflammation. After treatment with the TP/APR programmed system, the inflammatory cytokines in macrophages were decreased, and osteoclast activity was inhibited. Thus, fewer inflammatory cytokines were sensed by BMSCs, and at the same time, the APR released form the TP/APR programmed system promoted the osteogenic activity of BMSCs. As osteoimmune homeostasis was restored and osteogenesis was enhanced, bone regeneration in periodontitis-related alveolar bone defects commenced.

To further confirm the effects of the programmed delivery system, we constructed a periodontitis mouse model. In the presence of TP, fewer iNOS-positive macrophages were identified in the periodontal tissue, suggesting that TP can reduce inflammation, which is consistent with previous study [26]. Osteoclast activity is critical for bone regeneration [53]; in our study, TRAP staining revealed reduced TRAP protein secretion was observed in the TP and APR delivery groups, indicating that both TP and APR can inhibit osteoclastogenesis. The results of micro-CT indicated that the TP/APR sequential-release system resulted in the highest alveolar bone formation compared to the other groups. The

single-release nanofibers loaded with TP or APR showed mild therapeutic efficiency, which may be due to the regulation of inflammation or reducing of bone resorption. These results demonstrated that the TP/APR sequential-release system can create a favorable environment in the early stages and promote bone regeneration in later stages. In the *in vivo* experiment, no drug toxicity-related injury was found in animal organ samples, indicating that the doses of TP and APR are within a safe range. Hence, considering the *in vitro* and *in vivo* results in this experiment, we can conclude that the TP/APR released from the programmed-delivery system was present at effective concentrations.

To the best of our current knowledge, this is the first study to use a sequential and controlled release system to treat periodontitis-related alveolar bone defects. Compared with other treatment methods, the TP/APR programmed delivery system not only inhibits inflammation but also promotes bone regeneration. However, it is important to note that our results need to be confirmed in larger animal models. The current study verified the anti-inflammatory and bone regeneration-promoting effects of the TP-APR programmed delivery system. The periodontal ligament plays a crucial role in the health of periodontal tissues, and thus, future research focusing on regeneration of the periodontal ligament might be of interest [54,55]. Moreover, an evaluating of the degradation behavior of the TP-APR programmed delivery system for a longer time should also be considered. In the future, more sequential strategies matching the spatiotemporal specificity of periodontitis should be explored to achieve better outcomes.

5. Conclusion

In conclusion, the TP/APR programmed delivery system can promote bone regeneration in an inflammatory microenvironment, which mainly depends on the sequential effects of TP inhibiting the inflammation and APR promoting osteogenic differentiation. Considering the spatiotemporal specificity of periodontitis-related alveolar bone defects, the coordination between TP in the shell and APR in the core is necessary for bone regeneration. These findings reveal the TP/APR programmed delivery system has great applied potential in treating periodontitis-related alveolar bone defects.

Credit author statement

Z. He, contributed to conception, design, data acquisition, and analysis, drafted the manuscript: S. Liu, contributed to data acquisition and analysis, drafted the manuscript; Z. Li, contributed to conception and design, critically revised the manuscript; J. Xu, contributed to data acquisition and analysis, drafted the manuscript; Y. Liu, contributed to conception, design and data analysis, critically revised the manuscript; E. Luo, contributed to conception, design and data analysis, critically revised the manuscript.All authors gave final approval and agree to be accountable for all aspects of the work.

Declaration of competing interest

The authors declare that they have no known competing financial interests or personal relationships that could have appeared to influence the work reported in this paper.

Data availability

Data will be made available on request.

Acknowledgments

This study is supported by Grants from the National Natural Science Foundation of China (82001016; 81970917); Research and Develop Program, West China Hospital of Stomatology Sichuan University (RD-03-202102).

Appendix A. Supplementary data

Supplementary data to this article can be found online at https://doi.org/10.1016/j.mtbio.2022.100438.

References

[1] B.L. Pihlstrom, B.S. Michalowicz, N.W. Johnson, Periodontal diseases, Lancet (London, England) 366 (2005) 1809–1820.
[2] N.J. Kassebaum, E. Bernabé, M. Dahiya, B. Bhandari, C.J. Murray, W. Marcenes, Global burden of severe periodontitis in 1990-2010: a systematic review and meta-regression, J. Dent. Res. 93 (2014) 1045–1053.
[3] D.F. Kinane, P.G. Stathopoulou, P.N. Papapanou, Periodontal diseases, Nat. Rev. Dis. Prim. 3 (2017), 17038.
[4] N.H. Al-Rawi, N.K. Imran, A.A. Abdulkareem, A.M. Abdulsattar, A.T. Uthman, Association between Maternal Periodontitis, Acute-phase Reactants and Preterm Birth, Oral diseases, 2021.
[5] M. Sanz, A. Marco Del Castillo, S. Jepsen, J.R. Gonzalez-Juanatey, F. D'Aiuto, P. Bouchard, I. Chapple, T. Dietrich, I. Gotsman, F. Graziani, D. Herrera, B. Loos, P. Madianos, J.B. Michel, P. Perel, B. Pieske, L. Shapira, M. Shechter, M. Tonetti, C. Vlachopoulos, G. Wimmer, Periodontitis and cardiovascular diseases: consensus report, J. Clin. Periodontol. 47 (2020) 268–288.
[6] G. Hajishengallis, J.D. Lambris, Complement-targeted therapeutics in periodontitis, Adv. Exp. Med. Biol. 735 (2013) 197–206.
[7] P.M. Bartold, S. Gronthos, S. Ivanovski, A. Fisher, D.W. Hutmacher, Tissue engineered periodontal products, J. Periodontal. Res. 51 (2016) 1–15.
[8] F.M. Chen, Y. Jin, Periodontal tissue engineering and regeneration: current approaches and expanding opportunities, Tissue engineering, Part B, Reviews 16 (2010) 219–255.
[9] H.N. Tang, Y. Xia, Y. Yu, R.X. Wu, L.N. Gao, F.M. Chen, Stem cells derived from "inflamed" and healthy periodontal ligament tissues and their sheet functionalities: a patient-matched comparison, J. Clin. Periodontol. 43 (2016) 72–84.
[10] J. Huang, L. Liu, S. Jin, Y. Zhang, L. Zhang, S. Li, A. Song, P. Yang, Proanthocyanidins promote osteogenic differentiation of human periodontal ligament fibroblasts in inflammatory environment via suppressing NF-κB signal pathway, Inflammation 43 (2020) 892–902.
[11] T. Kwon, I.B. Lamster, L. Levin, Current concepts in the management of periodontitis, Int. Dent. J. 71 (2021) 462–476.
[12] S. Khorshidi, A. Solouk, H. Mirzadeh, S. Mazinani, J.M. Lagaron, S. Sharifi, S. Ramakrishna, A review of key challenges of electrospun scaffolds for tissue-engineering applications, Journal of tissue engineering and regenerative medicine 10 (2016) 715–738.
[13] Y. Liu, L. Liu, Z. Wang, G. Zheng, Q. Chen, E. Luo, Application of electrospinning strategy on cartilage tissue engineering, Curr. Stem Cell Res. Ther. 13 (2018) 526–532.
[14] X. Zhou, Q. Saiding, X. Wang, J. Wang, W. Cui, X. Chen, Regulated exogenous/endogenous inflammation via "Inner-Outer" medicated electrospun fibers for promoting tissue reconstruction, Advanced healthcare materials 11 (2022), e2102534.
[15] T. Wu, X. Mo, Y. Xia, Moving electrospun nanofibers and bioprinted scaffolds toward translational applications, Advanced healthcare materials 9 (2020), e1901761.
[16] Y. Zhang, T. Sun, C. Jiang, Biomacromolecules as carriers in drug delivery and tissue engineering, Acta Pharm. Sin. B 8 (2018) 34–50.
[17] D.N. Kapoor, A. Bhatia, R. Kaur, R. Sharma, G. Kaur, S. Dhawan, PLGA: a unique polymer for drug delivery, Ther. Deliv. 6 (2015) 41–58.
[18] N. Vázquez, F. Sánchez-Arévalo, A. Maciel-Cerda, I. Garnica-Palafox, R. Ontiveros-Tlachi, C. Chaires-Rosas, G. Piñón-Zarate, M. Herrera-Enríquez, M. Hautefeuille, R. Vera-Graziano, A. Castell-Rodríguez, Influence of the PLGA/gelatin ratio on the physical, chemical and biological properties of electrospun scaffolds for wound dressings, Biomed. Mater. (Bristol, U. K.) 14 (2019), 045006.
[19] Y. Li, Y. Xiao, C. Liu, The horizon of materiobiology: a perspective on material-guided cell behaviors and tissue engineering, Chem. Rev. 117 (2017) 4376–4421.
[20] Y. Su, B. Zhang, R. Sun, W. Liu, Q. Zhu, X. Zhang, R. Wang, C. Chen, PLGA-based biodegradable microspheres in drug delivery: recent advances in research and application, Drug Deliv. 28 (2021) 1397–1418.
[21] M. Feres, L.C. Figueiredo, G.M. Soares, M. Faveri, Systemic antibiotics in the treatment of periodontitis, Periodontology 67 (2015) (2000) 131–186.
[22] K. Jepsen, S. Jepsen, Antibiotics/antimicrobials: systemic and local administration in the therapy of mild to moderately advanced periodontitis, Periodontology 71 (2016) (2000) 82–112.
[23] B. Kouidhi, Y.M. Al Qurashi, K. Chaieb, Drug resistance of bacterial dental biofilm and the potential use of natural compounds as alternative for prevention and treatment, Microb. Pathog. 80 (2015) 39–49.
[24] A.B. Lagha, D. Grenier, Tea polyphenols protect gingival keratinocytes against TNF-α-induced tight junction barrier dysfunction and attenuate the inflammatory response of monocytes/macrophages, Cytokine 115 (2019) 64–75.
[25] Y. Li, X. Jiang, J. Hao, Y. Zhang, R. Huang, Tea polyphenols: application in the control of oral microorganism infectious diseases, Arch. Oral Biol. 102 (2019) 74–82.
[26] V.K. Chava, B.D. Vedula, Thermo-reversible green tea catechin gel for local application in chronic periodontitis: a 4-week clinical trial, J. Periodontol. 84 (2013) 1290–1296.

[27] T. Maruyama, T. Tomofuji, Y. Endo, K. Irie, T. Azuma, D. Ekuni, N. Tamaki, T. Yamamoto, M. Morita, Supplementation of green tea catechins in dentifrices suppresses gingival oxidative stress and periodontal inflammation, Arch. Oral Biol. 56 (2011) 48–53.
[28] R. Assuma, T. Oates, D. Cochran, S. Amar, D.T. Graves, IL-1 and TNF antagonists inhibit the inflammatory response and bone loss in experimental periodontitis, J. Immunol. 160 (1998) (1950) 403–409. Baltimore, Md.
[29] H.A. Lee, Y.R. Song, M.H. Park, H.Y. Chung, H.S. Na, J. Chung, Catechin ameliorates Porphyromonas gingivalis-induced inflammation via the regulation of TLR2/4 and inflammasome signaling, J. Periodontol. 91 (2020) 661–670.
[30] X. Wu, W. Qiu, Z. Hu, J. Lian, Y. Liu, X. Zhu, M. Tu, F. Fang, Y. Yu, P. Valverde, Q. Tu, Y. Yu, J. Chen, An adiponectin receptor agonist reduces type 2 diabetic periodontitis, J. Dent. Res. 98 (2019) 313–321.
[31] H. Liu, S. Liu, H. Ji, Q. Zhao, Y. Liu, P. Hu, E. Luo, An adiponectin receptor agonist promote osteogenesis via regulating bone-fat balance, Cell Prolif 54 (2021), e13035.
[32] H. Ji, Y. Wang, H. Liu, Y. Liu, X. Zhang, J. Xu, Z. Li, E. Luo, Programmed core-shell electrospun nanofibers to sequentially regulate osteogenesis-osteoclastogenesis balance for promoting immediate implant osseointegration, Acta Biomater. 135 (2021) 274–288.
[33] C. Ni, J. Zhou, N. Kong, T. Bian, Y. Zhang, X. Huang, Y. Xiao, W. Yang, F. Yan, Gold nanoparticles modulate the crosstalk between macrophages and periodontal ligament cells for periodontitis treatment, Biomaterials 206 (2019) 115–132.
[34] D. Du, Z. Zhou, L. Zhu, X. Hu, J. Lu, C. Shi, F. Chen, A. Chen, TNF-α suppresses osteogenic differentiation of MSCs by accelerating P2Y(2) receptor in estrogen-deficiency induced osteoporosis, Bone 117 (2018) 161–170.
[35] J. Liu, B. Chen, F. Yan, W. Yang, The influence of inflammatory cytokines on the proliferation and osteoblastic differentiation of MSCs, Curr. Stem Cell Res. Ther. 12 (2017) 401–408.
[36] Y.C. Pereira, G.C. do Nascimento, D.M. Iyomasa, M.M. Iyomasa, Muscle characterization of reactive oxygen species in oral diseases, Acta Odontol. Scand. 73 (2015) 81–86.
[37] E.A. Sallum, F.V. Ribeiro, K.S. Ruiz, A.W. Sallum, Experimental and clinical studies on regenerative periodontal therapy, Periodontology 79 (2019) (2000) 22–55.
[38] L. Roseti, V. Parisi, M. Petretta, C. Cavallo, G. Desando, I. Bartolotti, B. Grigolo, Scaffolds for bone tissue engineering: state of the art and new perspectives, materials science & engineering, C, Materials for biological applications 78 (2017) 1246–1262.
[39] Y. Mao, Y. Zhao, J. Guan, J. Guan, T. Ye, Y. Chen, Y. Zhu, P. Zhou, W. Cui, Electrospun fibers: an innovative delivery method for the treatment of bone diseases, Expet Opin. Drug Deliv. 17 (2020) 993–1005.
[40] Z. Wu, C. Bao, S. Zhou, T. Yang, L. Wang, M. Li, L. Li, E. Luo, Y. Yu, Y. Wang, X. Guo, X. Liu, The synergetic effect of bioactive molecule-loaded electrospun core-shell fibres for reconstruction of critical-sized calvarial bone defect-The effect of synergetic release on bone Formation, Cell Prolif 53 (2020), e12796.
[41] L. Jin, T. Wang, M.L. Zhu, M.K. Leach, Y.I. Naim, J.M. Corey, Z.Q. Feng, Q. Jiang, Electrospun fibers and tissue engineering, J. Biomed. Nanotechnol. 8 (2012) 1–9.
[42] C.E. Campiglio, N. Contessi Negrini, S. Farè, L. Draghi, Cross-Linking Strategies for Electrospun Gelatin Scaffolds, Materials, Basel, Switzerland), 2019, p. 12.
[43] S. Jin, X. Xia, J. Huang, C. Yuan, Y. Zuo, Y. Li, J. Li, Recent advances in PLGA-based biomaterials for bone tissue regeneration, Acta Biomater. 127 (2021) 56–79.
[44] M.G. Grewal, C.B. Highley, Electrospun hydrogels for dynamic culture systems: advantages, progress, and opportunities, Biomater. Sci. 9 (2021) 4228–4245.
[45] H. Newman, Y.V. Shih, S. Varghese, Resolution of inflammation in bone regeneration: from understandings to therapeutic applications, Biomaterials 277 (2021), 121114.
[46] Y. Chen, S. Cheng, J. Dai, L. Wang, Y. Xu, X. Peng, X. Xie, C. Peng, Molecular mechanisms and applications of tea polyphenols: a narrative review, J. Food Biochem. 45 (2021), e13910.
[47] A.C. Wu, L.J. Raggatt, K.A. Alexander, A.R. Pettit, Unraveling macrophage contributions to bone repair, BoneKEy Rep. 2 (2013) 373.
[48] Z. Jamalpoor, A. Asgari, M.H. Lashkari, A. Mirshafiey, M. Mohsenzadegan, Modulation of macrophage polarization for bone tissue engineering applications, Iran. J. Allergy, Asthma Immunol. 17 (2018) 398–408.
[49] S. Watanabe, M. Alexander, A.V. Misharin, G.R.S. Budinger, The role of macrophages in the resolution of inflammation, J. Clin. Invest. 129 (2019) 2619–2628.
[50] S. Gordon, F.O. Martinez, Alternative activation of macrophages: mechanism and functions, Immunity 32 (2010) 593–604.
[51] S.A. Hienz, S. Paliwal, S. Ivanovski, Mechanisms of bone resorption in periodontitis, Journal of immunology research (2015), 615486, 2015.
[52] Y. Niu, Z. Wang, Y. Shi, L. Dong, C. Wang, Modulating macrophage activities to promote endogenous bone regeneration: biological mechanisms and engineering approaches, Bioact. Mater. 6 (2021) 244–261.
[53] J.M. Kim, C. Lin, Z. Stavre, M.B. Greenblatt, J.H. Shim, Osteoblast-osteoclast communication and bone homeostasis, Cells (2020) 9.
[54] T. de Jong, A.D. Bakker, V. Everts, T.H. Smit, The intricate anatomy of the periodontal ligament and its development: lessons for periodontal regeneration, J. Periodontal. Res. 52 (2017) 965–974.
[55] A. Tomokiyo, N. Wada, H. Maeda, Periodontal ligament stem cells: regenerative potency in periodontium, Stem Cell. Dev. 28 (2019) 974–985.